80. Pollard, B.: Effect of Titanium on the Ductility of 26% Chromium Low Interstitial Ferritic Stainless Steel, *Met. Tech.*, January 1974, pp. 31–36.
81. Sipos, D. J., R. F. Steigerwald, and N. E. Whitcomb: Ductile Corrosion-resistant Ferrous Alloys Containing Chromium, U.S. Patent no. 3,672,876, Jun. 27, 1972.
82. Bond, A. P.: Effects of Molybdenum on the Pitting Potentials of Ferritic Stainless Steels at Various Temperatures, *J. Electrochem. Soc.*, vol. 120, no. 5, pp. 603–613, 1973.
83. Steigerwald, R. F.: Low Interstitial Fe-Cr-Mo Ferritic Stainless Steels, *Soviet-American Symp. New Developments in the Field of Molybdenum-alloyed Cast Iron and Steel*, Moscow, January 1973. Climax Molybdenum Co., Greenwich, Conn.
84. Steigerwald, R. F.: New Ferritic Stainless Steels to Resist Chlorides and Stress Corrosion Cracking, *Tappi*, vol. 56, no. 4, pp. 129–133, 1973.
85. Steigerwald, R. F.: New Molybdenum Steels and Alloys for Corrosion Resistance, *NACE preprint no. 44, 1974 Conf. Nat. Assoc. Corrosion Engineers*, Chicago.
86. Streicher, M. A.: Microstructures and Some Properties of Fe-28%Cr-4%Mo Alloys, *Corrosion*, vol. 30, no. 4, pp. 115–124, 1974.
87. McMullin, J. G., S. F. Reiter, and D. G. Ebeling: Equilibrium Structure in Fe-Cr-Mo Alloys, *Trans. Am. Soc. Met.*, vol. 46, pp. 799–811, 1954.
88. Aggen, G.: Unpublished work, Allegheny Ludlum Industries, Inc., Pittsburgh, Pa.
89. Demo, J. J.: Unpublished work, E. I. du Pont de Nemours & Co., Inc., Wilmington, Delaware.
90. Schmidt, W., and O. Jarleborg: Ferritic Stainless Steels With 17% Cr, Climax Molybdenum GmbH, Düsseldorf, Germany—An Affiliate of American Metal Climax, Inc., 1974.

Chapter 6

Structure and Constitution of Wrought Martensitic Stainless Steels

PAUL T. LOVEJOY
Research Metallurgist, Research Center, Allegheny Ludlum Steel Corporation, Brackenridge, Pennsylvania

CONSTITUTION

An austenitic field in the equilibrium diagram is one of the basic necessities for a martensitic stainless steel. The other necessity is that the chromium content be at or above

about 10.5 wt % so that the alloy can develop a "passive film" and display the good corrosion resistance expected of a stainless steel.

The extent of the gamma loop in the binary Fe-Cr system is seen in Fig. 1 developed by Baerlecken.[1] This indicates that some additonal element or combination of elements will be necessary to expand the austenitic field to usable stainless chromium levels. Figures 2 to 4 show the extent to which several austenite formers (carbon, nitrogen, nickel) expand the gamma loop. These latter diagrams do not indicate the extent of the two-phase α plus γ field.

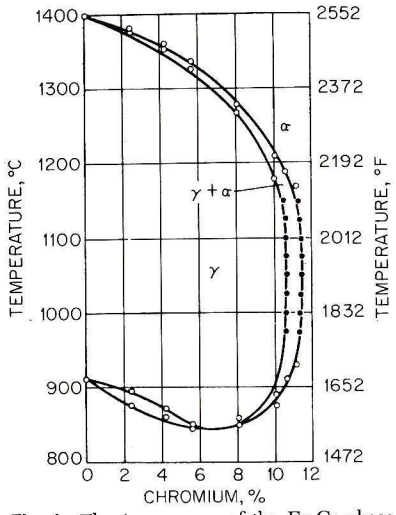

Fig. 1 The iron corner of the Fe-Cr phase diagram for alloys with approximately 0.004% C and 0.002% N.[1]

The extent of the two-phase region and carbide types is indicated in Figs. 5 to 7 attributed to Bungardt, Kunze, and Horne.[2] In these diagrams, the outer extent of the two-phase region is expanded but the single-phase field, necessary to achieve a uniform martensitic structure, is seen as not greatly changed.

Sections through the Fe-Cr carbon fields are shown in Fig. 8.[22] These show that as chromium increases, the single-phase austenite field decreases in area to the point where some primary carbides must be anticipated in several of the high-chromium—high-carbon alloys. Conversely, without carbon, the high-chromium steels could not be hardened.

For a specific 16Cr-2Ni alloy (Type 431), a phase diagram has been experimentally constructed as shown in Fig. 9.[3] This is compared with the theoretical diagram which was constructed from literature sources, Fig. 10. Comparisons indicate that the range for uniform hardening is considerably restricted in the real case. In order to ensure equilibrium it was found necessary in developing the diagram to use soaking times varying from ½ h at 2700°F (1468°C) to 500 h at 1200°F (634°C). This is due to the sluggish reaction kinetics in the Fe-Cr system.

Although specific phase boundaries are not presented, several authors[4,5] have shown that the austenite field may be expanded to alloys containing over 20% chromium if

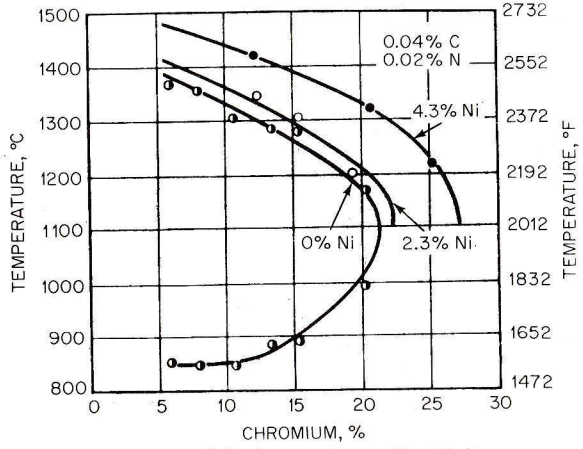

Fig. 2 Shift of gamma loop with nickel.[1]

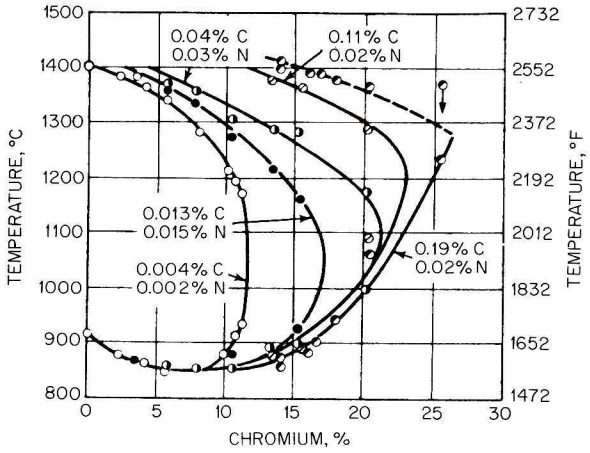

Fig. 3 Shift of gamma loop with carbon.[1]

sufficient nitrogen can be taken into solution. Dependent on heat treatment and chemistry, the austenite may be transformed or retained upon cooling. Lower temperature treatments may precipitate some carbides permitting martensite formation. The mechanism is depletion of matrix alloy content which raises the M_s temperature* for transformation.

Pseudo phase diagrams for a titanium stabilized martensitic steel have been presented by Kaltenhauser in Fig. 11.[6] These explain the behavior of a new type of maraging titanium-stabilized martensitic steel which does not require any tempering to achieve usable ductility levels at martensitic strength levels. Since the major portion of carbon is combined as a stable titanium carbide, there is no need for subsequent tempering.

Numerical Equivalents Useful engineering alloys usually contain more components than are represented on an equilibrium diagram. Thus for evaluation of structures in complex alloys various equivalent procedures have been developed. These are either equivalent procedures relating the effect of one element to that for a fixed amount of the

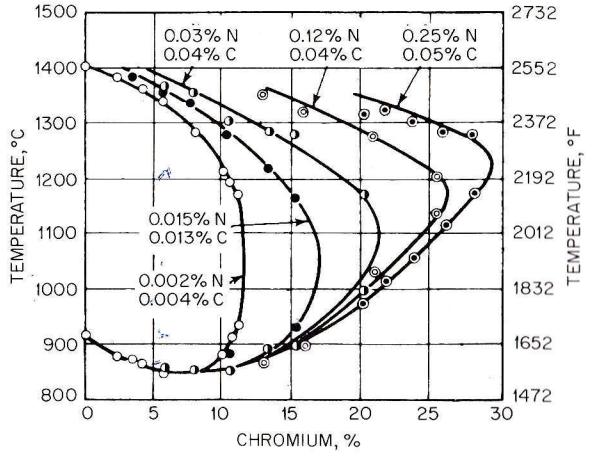

Fig. 4 Shift of gamma loop with nitrogen.[1]

*M_s means martensitic start.

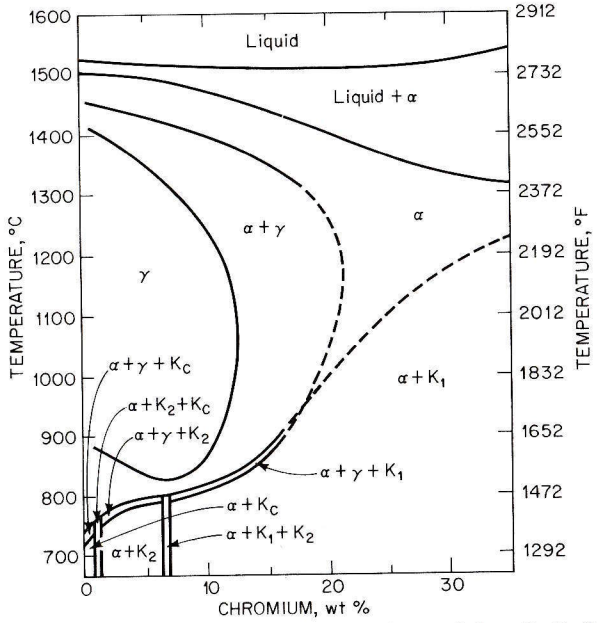

Fig. 5 Constant section at 0.05% carbon through Fe-Cr-C diagram.[2] K_c = Fe_3C; K_1 = $(Fe,Cr)_{23}C_6$; K_2 = $(Fe,Cr)_7C_3$.

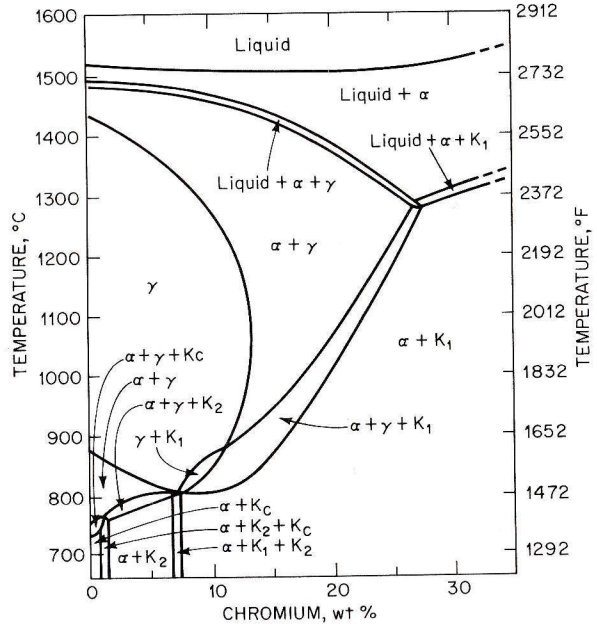

Fig. 6 Constant section at 0.10% carbon through Fe-Cr-C diagram.[2] K_c = Fe_3C; K_1 = $(Fe,Cr)_{23}C_6$; K_2 = $(Fe,Cr)_7C_3$.

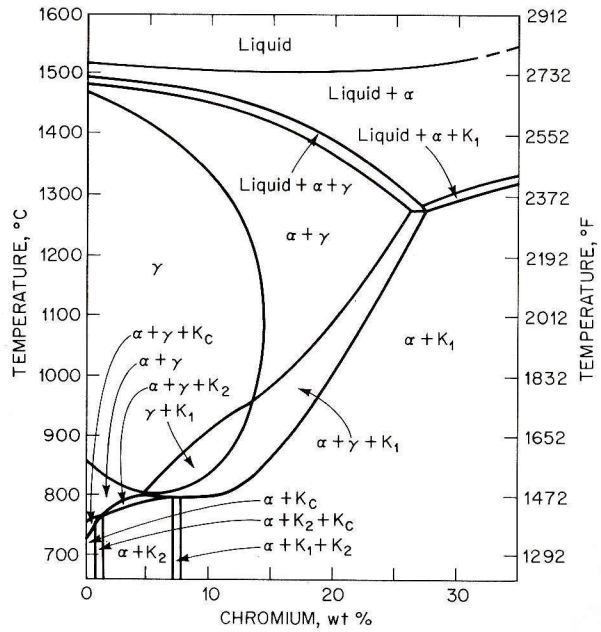

Fig. 7 Constant section at 0.20% carbon through Fe-Cr-C diagram.[2] K_c = Fe_3C; K_1 = $(Fe,Cr)_{23}C_6$; K_2 = $(Fe,Cr)_7C_3$.

standard or are relative potency factors. The utility is for general understanding and should not be solely relied on in specific cases.

Thielemann[7] provided one of the first formulations based on the ability of a particular element to close off the austenite field in an iron-based system. The applicable equation is

$$Cr_{Eq} = Cr + 2.1W + 2.8Ta + 4.2Mo + 4.5Cb + 5.2Si + 7.2Ti + 11V + 12Al - 40(C + N) - 3Ni - 2Mn$$

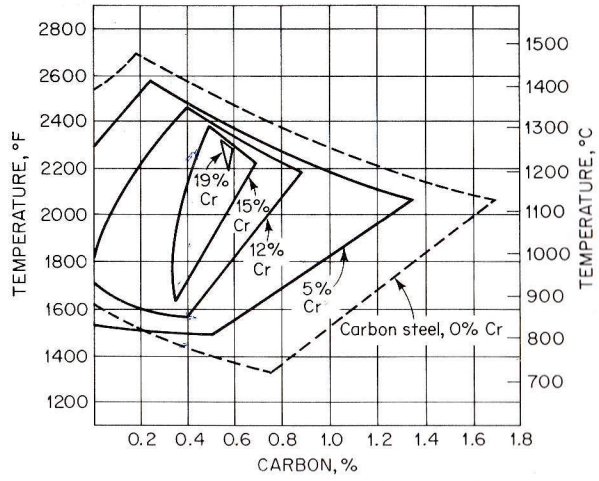

Fig. 8 Effect of several chromium contents on the carbon limitations for pure austenite at elevated temperatures.[22]

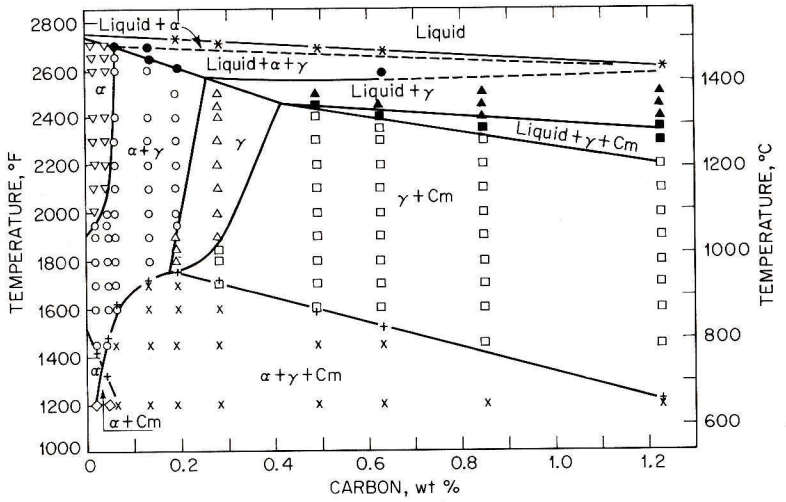

Fig. 9 Constitution diagram for 16Cr-2Ni stainless steel.[3] Symbol "Cm" indicates $(Cr,Fe)_{23}C_6$ and $(Cr,Fe)_7C_3$. Code: + = data derived from dilatometry;* = data derived from thermal analysis; all other data derived by metallographic examination.

These coefficients have been reestimated by Aggen[8] to include a 10 to 12% chromium base. This formulation is more applicable to martensitic stainless alloys:

$$Cr_{Eq} = Cr + 1.5Si + 7.2Ti + 2.5Al + 3Cb + 10Zr + 2V - 40(C + N) - 3Ni - 2(Mn + Cu)$$

Delta Ferrite The generally undesirable high-temperature bcc phase can occur in many martensitic stainless grades. The cause may be variation in chemistry or excessively high heat treatment.

The effects of chemistry on delta ferrite have been estimated by Irving.[9] For a fixed temperature of 1050°C, in a 12% Cr alloy having about 20% delta ferrite, the following factors were determined:

Change in Delta Ferrite, % per % Element	
N −220	Si +6
C −210	Mo +5
Ni −20	Cr +14
Co −7	V +18
Cu −7	Al +54
Mn −6	

Study of these effects in a 17Cr-4Ni base produced similar values. The carbide and nitride formers Ti and Cb were not evaluated but are known to be inherent ferrite formers and able to lessen the effects of carbon and nitrogen.

The effect of elevated temperature on delta ferrite is predicted by the phase diagram. Using a base composition of:

C	Mn	Si	Cr	N
0.1	0.5	0.25	12	0.02

Irving developed the following percentages of delta ferrite:

Temperature, °C	1050	1300	1350
% delta ferrite	0	50	100

Hence, delta ferrite may be dissolved or formed by heat treatment.

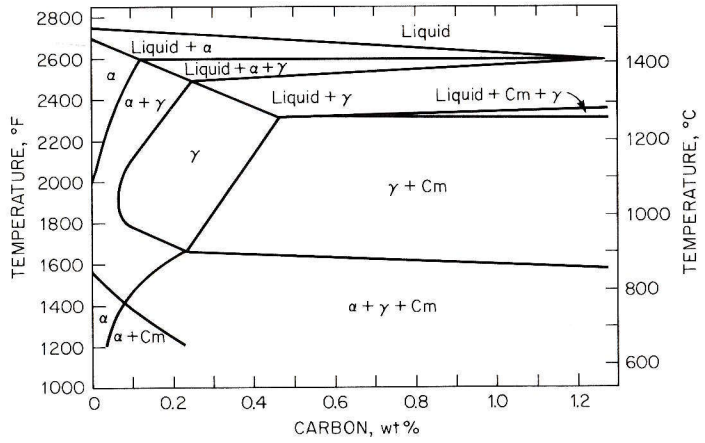

Fig. 10 16Cr-2Ni constitution diagram as extrapolated from literature.[3]

Decomposition of Delta Ferrite In simple Fe-Cr alloys delta ferrite will dissolve by the usual diffusional processes on first entering the austenite field. If retained to lower temperature, however, other phases may precipitate.

A. E. Nehrenberg and P. Lillys[4] have reported a study of the high-temperature transformations in 17 to 25% Cr steels. At high temperatures, delta ferrite transforms to austenite with all carbon taken into solution. At lower temperatures, however, they observed an aggregate of carbides in austenite. A lamellar microstructure is formed by the simultaneous growth of carbide and austenite into the delta ferrite. The temperature range for this transformation was found to bracket the A_3 from approximately 50°F (28°C) below to 200 to 300°F (111 to 166°C) above over a 17 to 25% chromium range.

The mechanism for the lamellar structure is given as initial carbide precipitation depleting the adjacent matrix of both chromium and carbon. While the carbon will diffuse quickly, a chromium gradient is formed which adjusts the local chemistry to the left, into a stable austenite region. This austenite is then either stable or unstable during cooling depending on its M_s temperatures.

As an interesting aside, Tisinai and Samans[5] have shown that lamellar ferrite may form from austenite decomposition in high chromium, carbon, and nitrogen alloys through the precipitation of carbides and nitrides.

Other work on delta ferrite decomposition in a more complex alloy (AM-350, AM-355) has been reported by Aggen.[10] This alloy, which contains Mo in addition to Fe, Ni, Cr, C, and N, demonstrates a sequence of delta ferrite dissolution as shown in Figs. 12 to 14. These photomicrographs indicate that the precipitation of austenite, carbides, and chi phase may all be encountered.

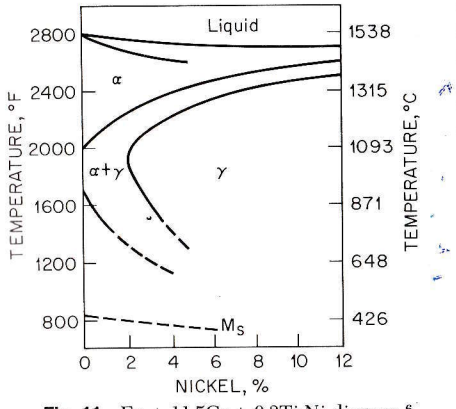

Fig. 11 Fe + 11.5Cr + 0.3Ti:Ni diagram.[6]

The dissolution of the delta ferrite depends on the matrix. If quenched directly into the carbide precipitation range, the decomposition proceeds mainly through the formation of austenite and carbides. The particles first form at the ferrite-austenite boundary. Later there is cellular growth of both austenite and carbide plates into the delta ferrite particles.

If the austenite is first transformed to martensite, the availability of carbon is diminished by precipitation in the matrix.

The ferrite is then decomposed as seen in Figs. 12 to 14. At lower temperatures of 1100 and 1250°F (580 to 662°C), distributed fine particles of austenite appear within the delta ferrite grains. There may also be carbide films formed at the austenite-ferrite boundary.

In the range of 1425 to 1600°F (761 to 857°C) decomposition proceeds mainly through the formation of austenite and massive particles of chi phase at the boundaries. Small amounts of sigma are also observed. At higher temperatures of 1750 to 1800°F (908 to 968°C), less chi and more sigma is formed. If the molybdenum were absent, the molybdenum-rich chi phase would likely be replaced by sigma phase.

Under unusual circumstances delta ferrite has been observed to transform at temperatures as low as 500 to 700°F (260 to 371°C). Dulis[11] has observed that Type 410 with 20% delta ferrite had better fatigue strength at 500°F (260°C) than at room temperature. This was attributed to precipitation of a finely distributed dispersion of alpha prime. The necessary enhanced precipitation rate is attributed to the vacancies and dislocations generated during the reversed plastic deformation.

Sigma Phase The low chromium of the martensitic stainless grades generally ensures that sigma phase does not form during elevated temperature exposure. At lower temperatures, however, the Fe-Cr miscibility gap can result in the precipitation of alpha prime which is given as the cause of 885°F embrittlement.

If severe cold-work (95%) is utilized to enhance the reaction, sigma has been identified in 14% Cr steels heated for 10,000 hr at 900°F (471°C).[12] At 5000 hr, there was no sigma present so that in most real situations sigma is not a credible consideration for martensitic steels. Long before sigma the utility would be lost due to 885°F (474°C) or temper embrittlement.

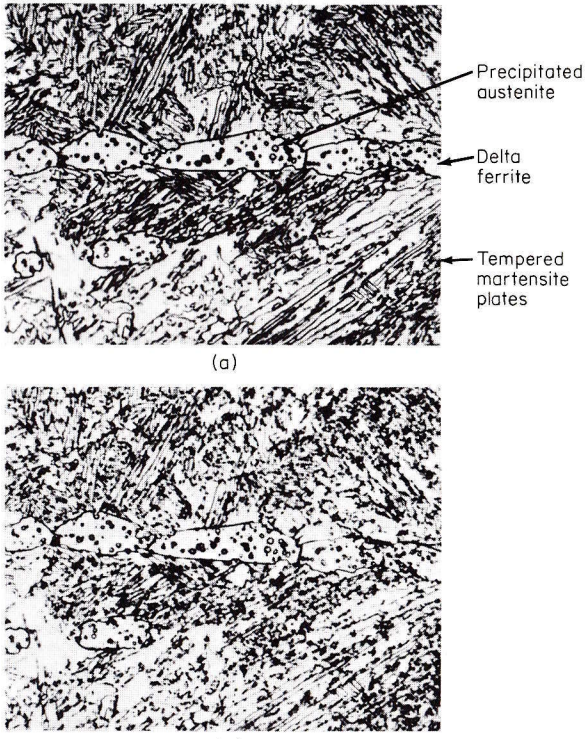

Fig. 12 Delta ferrite microstructure in AM-355 following 1950°F (1063°C) + water quench + subzero cooled + 1250°F (675°C), 16 h. Shows precipitation of austenite in ferrite. (*a*) Sodium hydroxide etchant. (*b*) Reetched in oxalic acid. 2000X.[10]

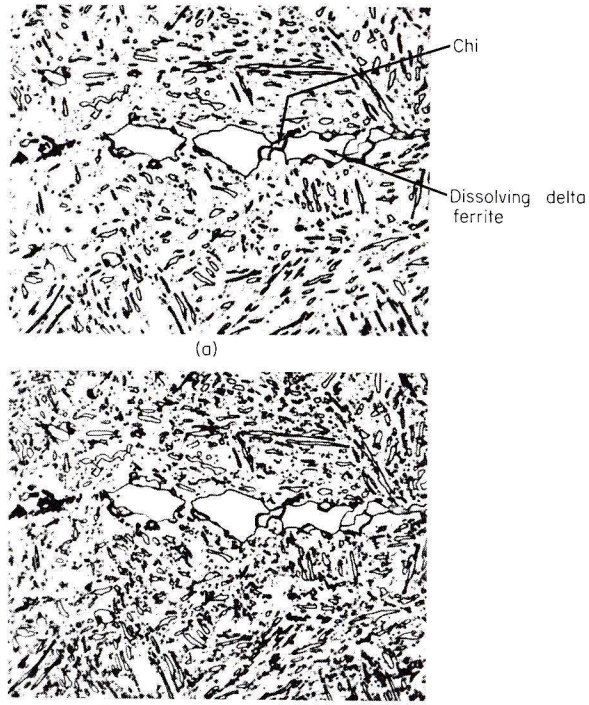

Fig. 13 Delta ferrite microstructure in AM-355 following 1950°F (1063°C) + water quench + subzero cooled + 1425°F (774°C), 16 h. Shows precipitation of austenite + chi in ferrite. (*a*) Sodium hydroxide etchant. (*b*) Reetched in oxalic acid. 2000X.[10]

STRENGTHENING MECHANISMS

In martensitic stainless steels strength implies not only the conventional flow stress for plastic deformation, but also hardness or abrasion resistance. These strength properties are determined by both the chemical makeup and the prior heat treatment.

Chemical Analysis The most obvious strengthening mechanism is the martensite reaction. The two main chemical factors which are important are the stability of delta ferrite at the hardening temperature and the carbon content. The delta ferrite equilibrium has already been discussed.

TABLE 1 Approximate Maximum Hardness

Alloy AISI	Carbon %	Hardening temperature	As-quenched hardness, R_c
410	0.115	1700°F (927°C) ½ h	44
		1850°F (1010°C) ½ h	44.5
414	0.13	1700°F (927°C) ½ h	44
		1900°F (1038°C) ½ h	44
431	0.14	1700°F (927°C) ½ h	42
		1900°F (1038°C) ½ h	41
420	0.31	1700°F (927°C) ½ h	49
		1875°F (1024°C) ½ h	52
440C	1.0	1700°F (927°C) 1 h	52
		1900°F (1038°C) 2 h	55

Carbon Content The trend of strength versus carbon content can be observed in the preceding table which lists the approximate maximum hardness versus alloy and carbon content.

These values indicate that higher carbon produces greater hardness until a saturation is reached at about the 0.60 carbon level in Type 440A. At this level, the austenite is saturated in carbon and further carbon is precipitated from the melt as primary carbides. These larger carbides do not enter into the hardening process, but do provide additional abrasion resistance.

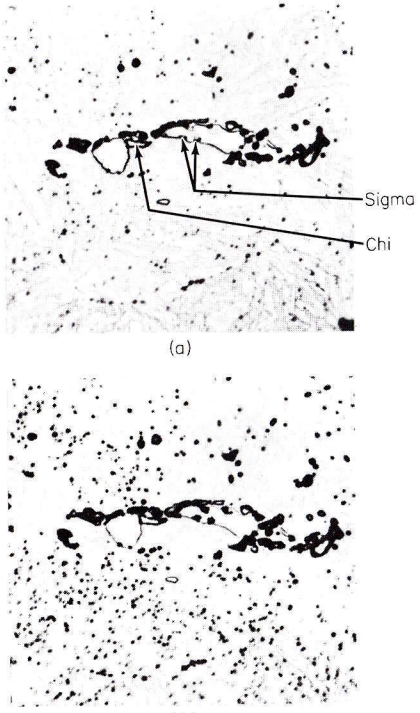

Fig. 14 Delta ferrite microstructure in AM-355 following 1950°F (1063°C) + water quench + subzero cooled + 1800°F (981°C), 16 h. Shows precipitation of austenite and sigma in ferrite. *(a)* Sodium hydroxide etchant. *(b)* Reetched in oxalic acid. 2000X.[10]

Other elements which are added to martensitic steels do not have the direct effect on strength that can be attributed to carbon. Their influence is usually indirect through control over phase stability, that is, relative austenite-ferrite stability at elevated temperature and the stability of austenite on cooling.

Cold-Working The deformation of annealed martensitic stainless steels will raise strength but the data presented in Table 2 suggest that heat treatment is a more effective method to raise strength. Note the precipitous drop in elongation with only small reductions.

Although cold reduction is not suitable as a final process for Type 410, the data do indicate that considerable deformation can be utilized in fabrication with final properties developed by heat treatment.

Hardenability The element chromium is known to greatly increase the hardenability of martensitic steels. This effect is used in many low-alloy steels. At the chromium levels necessary for a steel to be labeled stainless, the effect has saturated such that a Jominy End-Quench Hardenability Test will show no variation in hardness. Figure 15 shows TTT and E-Q curves for Type 410.

These diagrams suggest that it will be difficult to anneal these stainless steels to a soft ferrite plus carbides. Most softening attempts are better approached as over-

TABLE 2 The Effect of Cold-Work on Annealed Type 410

COMPOSITION:	C	Mn	Si	S	P	Cr	Ni
	0.10	0.44	0.349	0.016	0.017	12.18	0.405

Reduction	Yield strength MN/m²	Yield strength ksi	Ultimate tensile strength MN/m²	Ultimate tensile strength ksi	Elongation in 2 in. (50.8 mm), %	Hardness, R_b
0	256.5	37.2	493	71.5	30	72
15	634.3	92.0	648.1	94.0	6.5	95
30	724	105.0	751.6	109.0	2.5	99
45	758.5	110.0	806.7	117.0	1.0	100
60	827.4	120.0	882.6	128.0	1.0	100

tempering operations. This is particularly true in those martensitic steels containing nickel. Figure 16 shows the retarding that can occur with nickel in Type 414. The additional nickel stabilizes austenite up to one day at temperature.

Martempering There is sufficient hardenability in all martensitic stainless steels to permit martempering as a means to avoid cracking in complex heat-treated parts. The M_s measurements may be consulted to select appropriate quenching temperatures.

A typical martempering cycle could be constructed on Fig. 15 by cooling at a rate sufficient so as not to intersect the nose of the ferrite transformation curve, that is, 1300°F (704°C) at 200 s and not below the M_s of 680°F (360°C). This could be accomplished by quenching into a salt pot at the appropriate temperature. When the part reached a uniform temperature above the M_s, it could be cooled through the transformation range to martensite. This procedure greatly reduces the thermal strains and the danger of cracking.

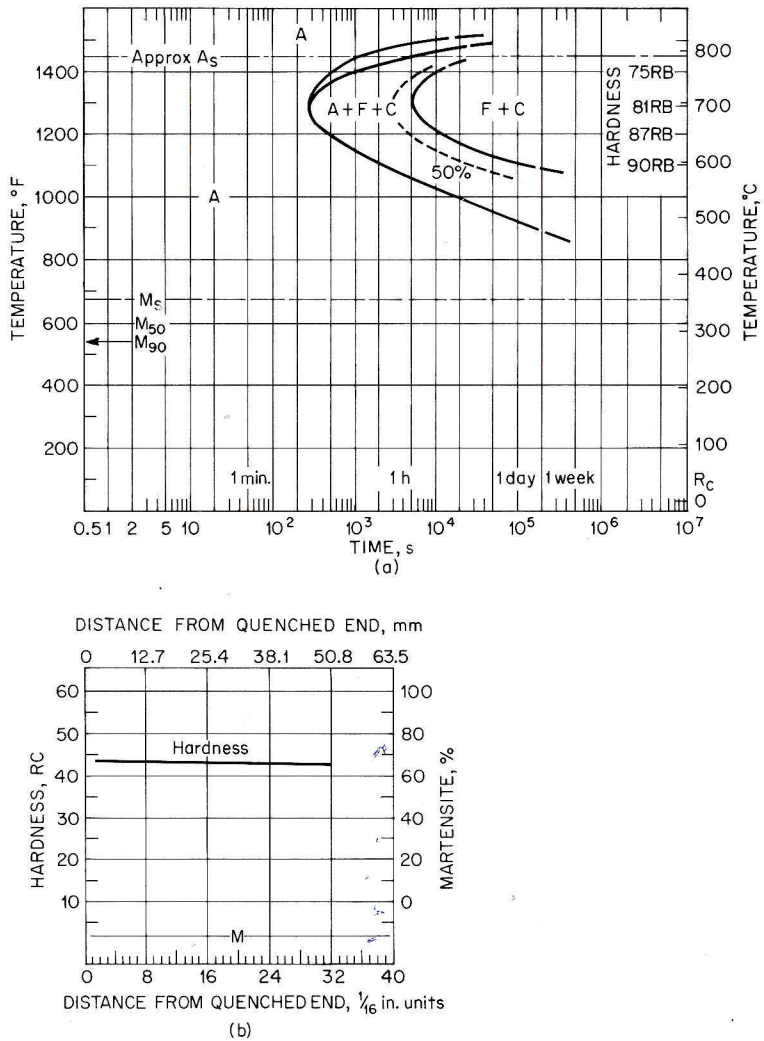

Fig. 15 *(a)* TTT diagram. *(b)* End-quench hardenability diagram for Type 410 stainless steel. Type 410 contains 0.11C-0.44Mn-0.37Si-0.16Ni-12.18Cr. Austenitized at 1800°F (981°C); grain size, 6–7. A, austenite; F, ferrite; C, carbide; M, martensite; B, bainite; P, pearlite.[20]

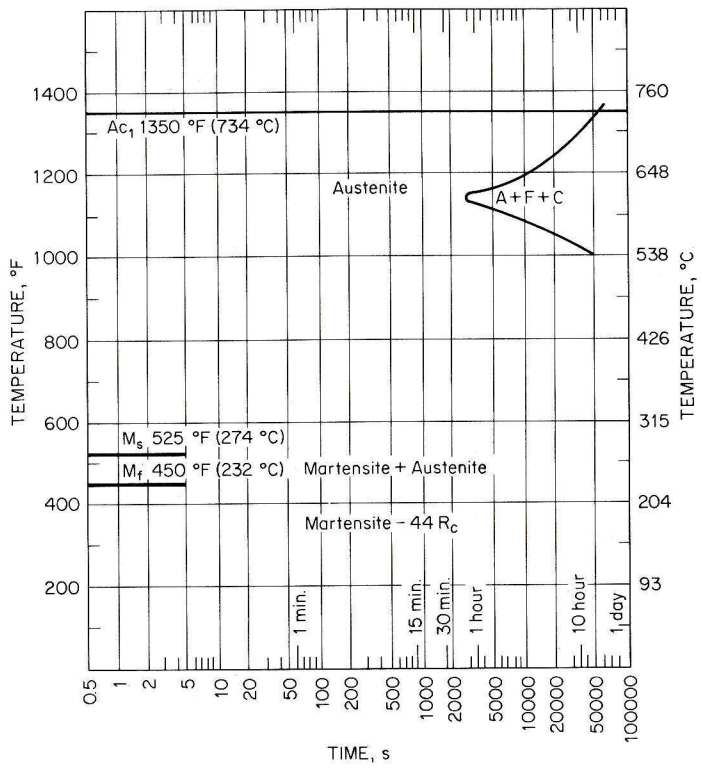

Fig. 16 TTT diagram for Type 414 stainless steel.[21]

Ausworking Deformation of metastable austenite prior to transformation produces significant improvement in the strength and toughness of many steels. These techniques are not, however, greatly utilized in martensitic stainless steels. The lower carbon grades have only a minimal response due to the minor carbide reaction while the higher grades are generally employed where high hardness and abrasion resistance are of primary concern. As a result, there is little information available. In the precipitation-hardening grades, ausworking can be utilized to improve strength and toughness.[13,14] A typical ausworking cycle would be much like the martempering cycle previously discussed. That is, the part is cooled to below the nose of the ferrite transformation as shown in Fig. 15. The metastable austenite is then worked or deformed at this lower temperature where more time is necessary for ferrite transformation. The austenite is then strengthened prior to martensite transformation. The martensite transformation is allowed to occur by cooling after the plastic deformation.

The effect of ausworking Type 410 at 800°F (427°C) is shown in Figs. 17 and 18.[15] These show that strength properties can be raised with some attendant loss in ductility values.

If plastic working is continued after the martensite transformation, then, as the values in Fig. 19[15] show, there can be a substantial increase in strength but a greater loss in ductility levels.

STRENGTHENING MECHANISMS IN LOW-CARBON MARTENSITES

Residual stress, solid-solution hardening, and prior austenite grain size are all factors in determining the strength of a martensite structure. These have been discussed using low-carbon nickel and chromium martensites.[16]

Residual Stress The level of residual stress is strongly related to the M_s temperature for two basic reasons. First, the volume discrepancy between austenite and ferrite increases as the metastable temperature range increases. Secondly, as the M_s decreases, there is less opportunity for autotempering.

These effects are demonstrated in Fig. 20[16] where the lower M_s steels show the greatest rise in proportional limit with tempering at 797°F (425°C). Note that the effect is stronger at lower temperatures.

Solid-Solution Strengthening Using the same alloys, the solid-solution strengthening due to nickel and chromium has been demonstrated as shown in Fig. 21.[16] Again, note that lower temperatures are necessary to demonstrate the effect. These rates are much less than those normally associated with solid-solution strengthening in a ferritic lattice.

Prior Austenite Grain Size The low carbon content of Floreen's alloys permits an estimate of grain-size effects obtained through heat treatment without corresponding variations in carbide solutioning. These values are shown in Fig. 22.[16]

The results follow the expected Petch relationship. Note, however, that the slope, or Petch constant, k_f is less than normally associated with ferritic steels.

MICROSTRUCTURE AND EFFECTS OF HEAT TREATMENT

Metallography The carbon content may be utilized to separate microstructures of martensitic steels into three categories:

- Class I, Low Carbon: Needlelike structure
- Class II, Medium Carbon: Very fine needlelike structure
- Class III, High Carbon: Ultra fine structure, contains primary carbides

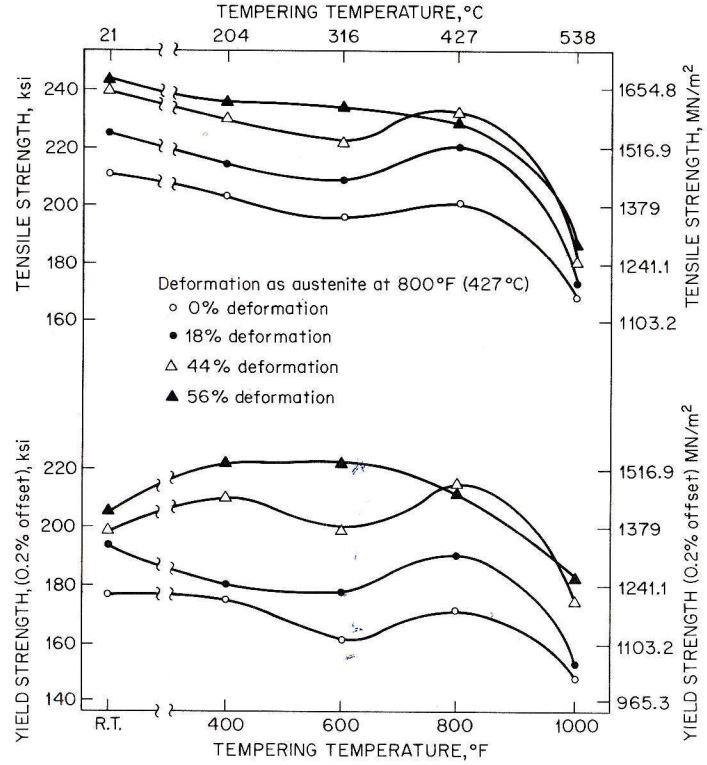

Fig. 17 The effect of tempering temperature on the tensile and yield strengths of Type 410 stainless steel deformed in the metastable austenitic condition.[15]

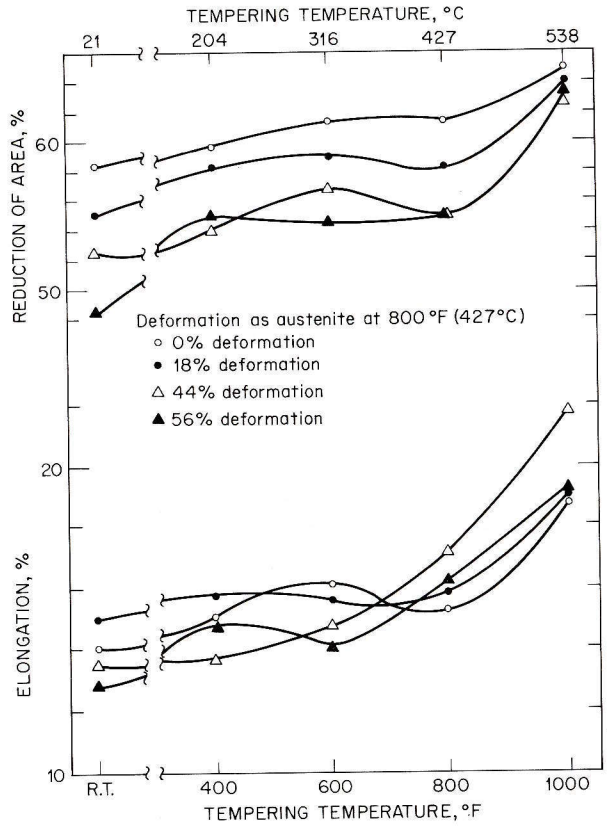

Fig. 18 The effect of tempering temperature on the reduction of area and elongation of Type 410 stainless steel deformed in the metastable austenitic condition.[15]

Structures representative of these three classes are shown in Fig. 23 in the hardened and tempered condition. In the first column the needlelike characteristic is visible. During a subcritical anneal, the needlelike structure is eliminated and visible carbides are precipitated, mostly in grain boundaries.

In the Type 420, the hardened structures have a similar appearance at low magnification.

Primary undissolved carbides are the principal constituents seen in the microstructures of the Type 440A high-carbon grades. In the annealed condition, both primary and secondary carbides can be observed as seen in Fig. 24. When hardened, the secondary carbides are taken into solution with a smaller percentage left to precipitate on grain boundaries as seen in Figs. 25 and 26.

Note the importance of the etching medium. The ammonium persulfate clearly outlines the carbide matrix boundaries, while the mixed acid etch develops additional matrix structure.

Hardening Treatments Forming an austenitic structure is the first prerequisite to achieving satisfactory properties. The factors of concern are the rate of heating and cooling, maximum temperature, and atmosphere.

The rate of heating is usually designed so that the part may be brought to a uniform temperature prior to the allotropic transformation. This is most important with heavy sections in the higher carbon grades. Occasionally a lower temperature hold at 1100°F (593°C) may be employed to further reduce strains.

The maximum temperature is determined by the need for maximum hardness. The data

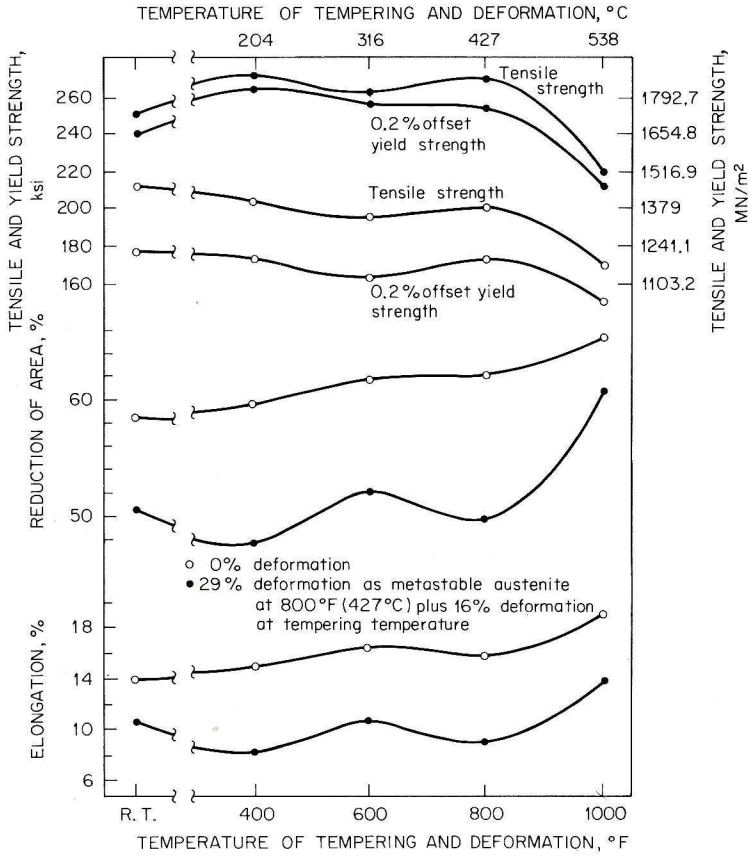

Fig. 19 The effect of deformation before and after martensite transformation on the tensile properties of Type 410 stainless steel. Steels deformed as metastable austenite to the indicated degree at 800°F (426°C), and worked as stated at the indicated temperatures after transformation.[15]

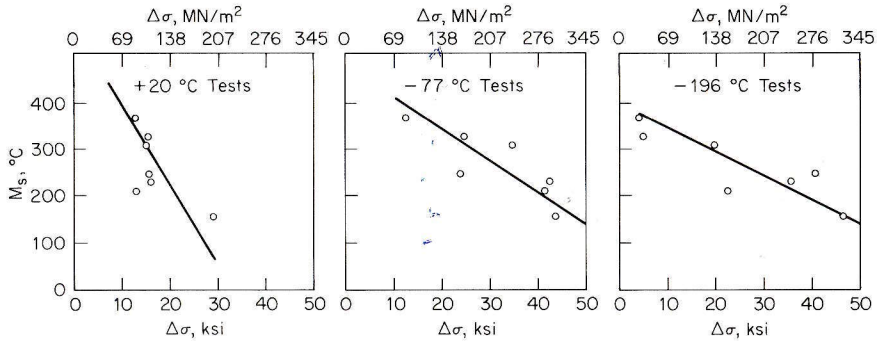

Fig. 20 Change in proportional limit after tempering at 425°C vs. M_s temperature. ($\Delta\sigma$ = 0.02% offset stress as tempered minus 0.02% offset stress as annealed.)[16]

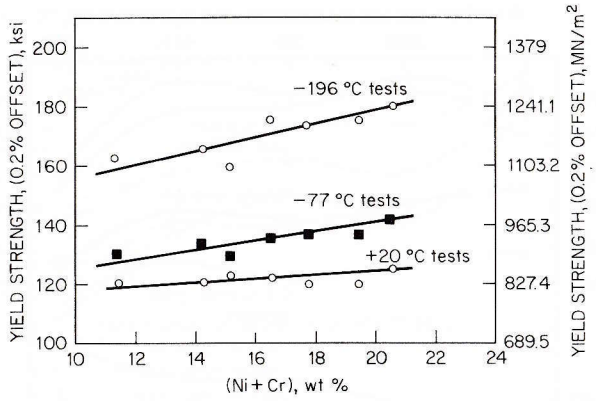

Fig. 21 Yield strength vs. total nickel plus chromium contents. Specimens tempered at 425°C.[16]

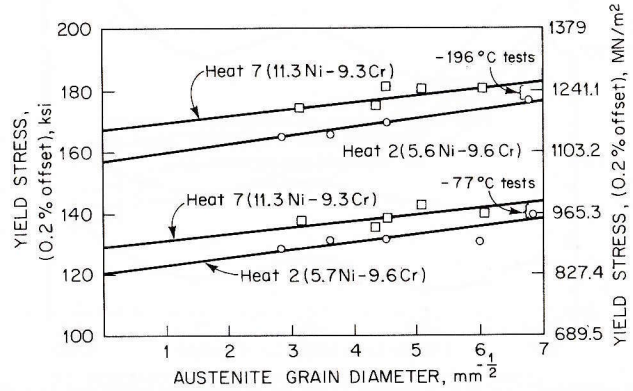

Fig. 22 Yield strength vs. reciprocal square root of prior austenite grain diameter.[16]

previously shown for Types 410, 420, and 440A illustrate the role of higher temperatures as well as the role of carbon in the attainment of greater hardness.

Heating in air can lead to surface decarburizing as shown by carbon content versus time and temperature in Table 3. The drop in bulk carbon depends on gage but note in these data the greatly reduced hardness in light-gage cutlery stock.

TABLE 3 Decarburization During Hardening

	Atmosphere			
	Air		Nitrogen	
Heat treatment	% C	Hardness, R_c	% C	Hardness, R_c
Type 410, gage 0.033 in. (0.84 mm):				
1900°F (1036°C) for 10 min, air-cooled	0.14	45.0	0.13	45.5
1900°F for 60 min, air-cooled	0.059	33.0	0.14	45.5
2100°F (1149°C) for 10 min, air-cooled	0.076	40.5	0.14	46.0
2100°F for 60 min, air-cooled	0.006	97.5R_b	0.12	45.0
Type 420, gage 0.066 in. (1.68 mm):				
1900°F for 10 min, air-cooled	0.39	57.0		
1900°F for 60 min, air-cooled	0.26	48.0		
2100°F for 10 min, air-cooled	0.33	56.5		

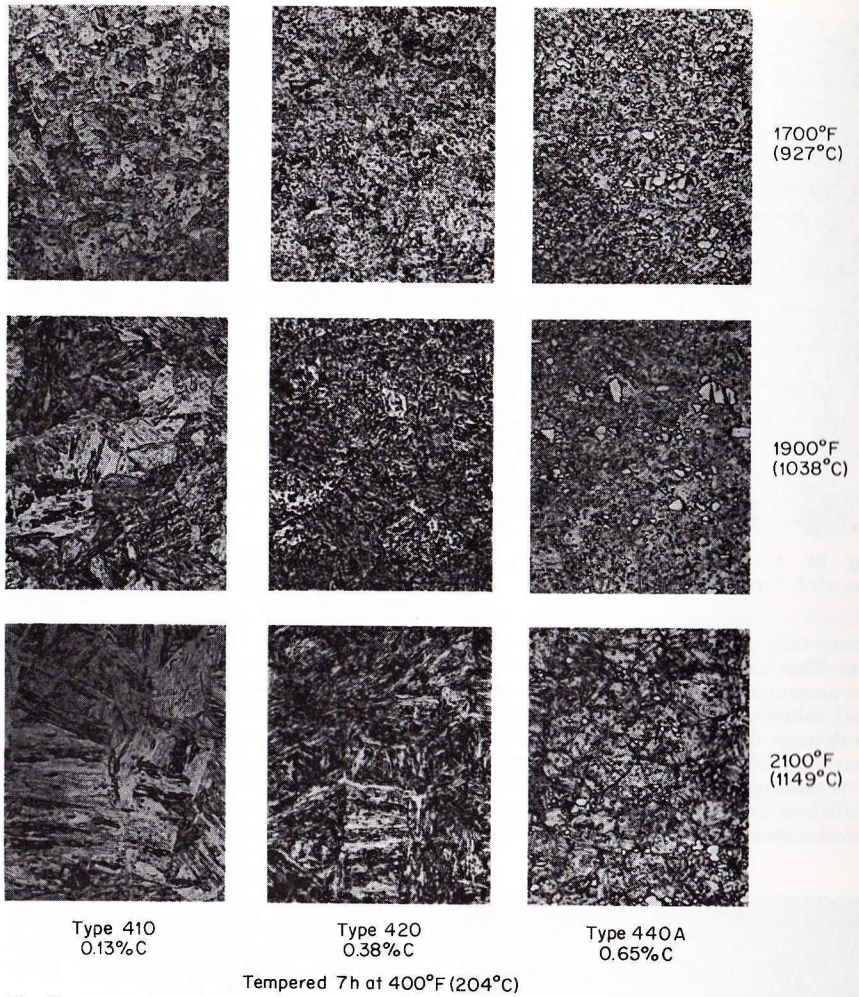

Fig. 23 Microstructures of hardened and tempered martensitic stainless steels as a function of carbon content. 500X.

The carbon loss may be reduced by heating in a nitrogen atmosphere. Note, however, that nitrogen may be absorbed and stabilize the austenite against transformation. Type 440A overheated to 2100°F (1149°C) for 10 min in nitrogen contained 94% retained austenite.

The $M_{23}C_6$ carbide begins to nucleate about 900°F (482°C) and becomes predominant above 1000°F (538°C). These carbides tend to be too large to influence strength and, additionally, are stable enough to significantly reduce the matrix carbon content which remained high during the lower temperature temper treatments. The net effect is the observed drop in hardness seen in all grades.

The chromium content of the precipitates may be followed in Fig. 28*a*. Note that chromium content is low until the more complex carbide types begin to form.

Rate of Cooling The great hardenability contributed by chromium removes the need to quench to avoid the formation of softer transformation products. It is possible, however, to precipitate sufficient carbide on cooling that both the M_s and the as-quenched hardness are influenced.

Data in Fig. 27 show that the cooling rate influences M_s only at higher carbon levels

Fig. 24 Ammonium persulfate, 1500X, box annealed, Type 440A, R_b 95.

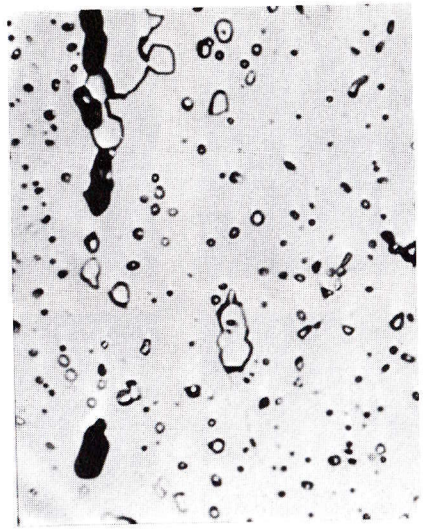

Fig. 25 Ammonium persulfate, 1500X, box annealed, +1950/2000°F (1063/1093°C), ½ h, +−125°F (−81°C), 1½ h, +350°F (177°C), 2 h, R_c 60.

above 0.20. Note that absolute hardening temperature becomes a factor before quench rate. That is, the higher hardening temperature dissolves a greater amount of carbide into the austenite structure. This carbide may reprecipitate before martensite transformation if the cooling is sufficiently slow and the already-precipitated carbon would not be available to depress the M_s or raise hardness. The effect is minor in most practical cases. The maximum observed hardness variation is from 50 to 45 R_c for holding times of 1 h.

Tempering In the as-hardened condition, martensitic stainless grades do not have sufficient toughness for engineering utility. For this reason, as with less-alloyed martensitic steels, a lower temperature heat treatment is utilized to restore toughness.

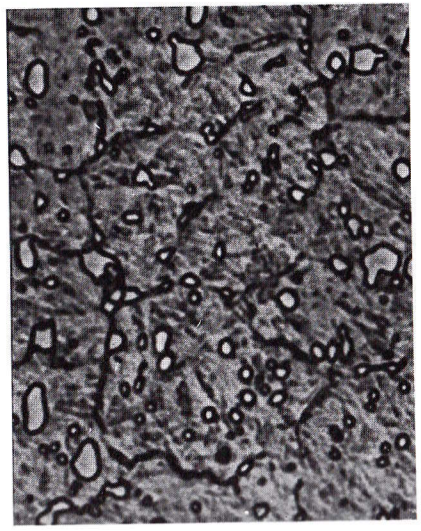

Fig. 26 Mixed acid etch, 2000X, hardened and tempered Type 440A.

With stainless steel there is an additional requirement to maintain corrosion resistance. Hence, it is necessary to discriminate between the higher chromium steels such as 440(ABC) and 420 and the remaining lower chromium varieties.

The higher chromium grades are usually selected with corrosion resistance in mind. This property would be adversely affected by high-temperature tempering (chromium carbide precipitation) and so these grades are usually stress-relieved at a lower temperature. Other stainless grades may be stress-relieved or tempered depending on the desired final properties.

Several reactions occur during tempering of martensitic steels. These are stress relief, previously mentioned, and a progression of carbide types tending toward more complex formulations. In the precipitation-hardenable grades there is additional precipitation of a fine dispersion of intermetallic carbides which provides additional strength.

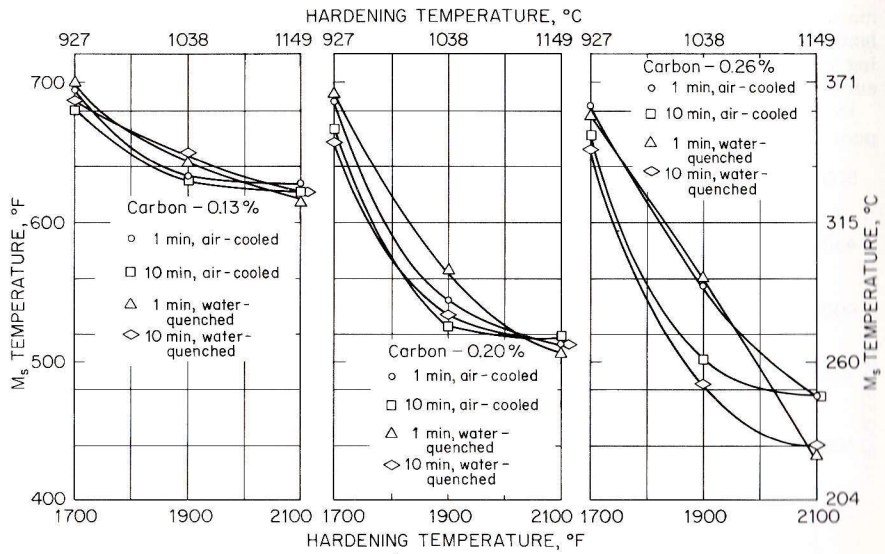

Fig. 27 Effect of solution, time, and cooling rate on M_s temperature.

The sequence of carbide reactions has been determined in Type 410 as seen in Fig. 28.[17] As-quenched, there is a fine dispersion of M_3C cementite-type carbides. These grow until at 600°F (315°C) the morphology changes from dendritic to platey-Widmanstätten distribution. At this temperature there is a slight contraction in length.

At higher temperatures, near 900°F (482°C), the M_7C_3 carbide becomes stable. These carbides may originally precipitate or may develop from favorably disposed elemental carbides. The maximum chromium in M_7C_3 is near 50% as opposed to the 18% maximum chromium in M_3C, hence the reduced corrosion resistance of martensitic grades tempered at this temperature is likely the result of a 3XX chromium-depletion mechanism.

The effect of tempering on hardness may be followed through the construction of a

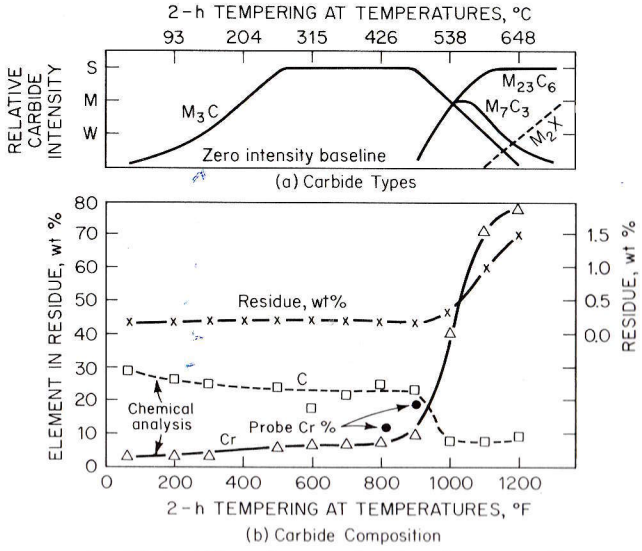

Fig. 28 Carbide analyses as a function of tempering.[17]

master tempering curve as shown in Fig. 29.[9] These show that the principal drop in hardness is associated with the precipitation of the $M_{23}C_6$ carbide. If a secondary hardening reaction exists, then the hardness would be expected to diverge from this master curve.

In practice the tempering range around 885°F (475 to 550°C) is not utilized due to the poor toughness of all martensitic stainless steels treated in this region. The reasons for the

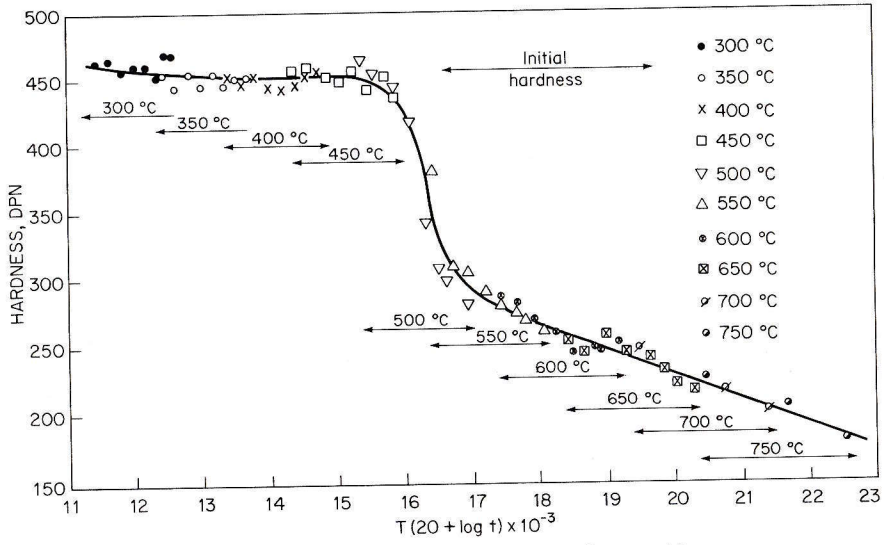

Fig. 29 Tempering curve for 0.14C-12Cr base steel.[9]

trough in toughness shown in Fig. 30[20] can be associated with the microstructural changes that are occurring in this region and with the possibility of temper embrittlement.

The principal microstructural changes are secondary hardening due to coherency strains from precipitates forming in the grain boundaries and overaging at the grain boundaries. This produces a structure which would be expected to be susceptible to brittle fracture. Additions of molybdenum or columbium,[18] the latter as shown in Fig. 31, can improve the toughness of martensitic steels in this area but the basic detrimental mechanisms remain.

Martensite Transformation Temperatures The heat treatment of highly alloyed stainless steels requires more consideration of the martensite transformation temperature (M_s) than is necessary in other martensitic steels. In many of the precipitation and semiaustenitic grades a subzero treatment is necessary to complete transformation. In the martensitic stainless grades, the formation of enriched and therefore retained austenite in high-temperature tempering operations is a phenomenon that occurs through depressing the M_s temperature with greater alloy content.

The effects of several elements on both the A_{c1} and M_s temperatures have been given by Irving.[9] For a 12% chromium base these are given by Table 4.

Another calculation for the A_{c1} temperature is offered by Tricot and Castro[19] as follows:

$$A_1\ (°C) = 310 + 35Cr + 3.5(Cr\text{-}17)^2 + 60Mo + 73Si + 170Cb + 290V + 620Ti + 750Al + 1400B - 250C - 280N - 115Ni - 66Mn - 18Cu$$

The difference in coefficients is due to using a 17% chromium base point.

The range of martensite transformation is about 150°C (270°F) or less. Hence, it is obvious that the minimum desirable M_s would be in the order of 200°C (392°F) to assume transformation on cooling to room temperatures.

One effect of the low M_s temperatures of the stainless grades is the small autotempering that can occur as the transformed martensite cools to room temperature. Hence, at

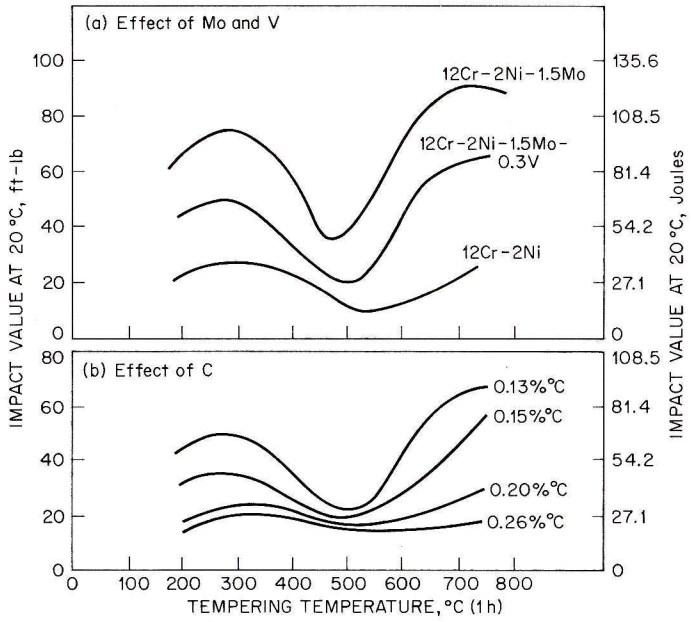

Fig. 30 Effect of tempering on impact properties of 12% Cr steels.[20]

equivalent carbon content, stainless grades may be slightly harder than corresponding carbon steels.

Retained Austenite The austenitic structure can be retained in any operation that may lead to enrichment of the matrix with any element capable of reducing the M_s temperature. This may occur either through external contamination prior to heat treatment or by improper heat treatment leading to internal segregation. Typical mechanisms are listed below.

Higher-than-recommended hardening temperatures may dissolve an excessive amount

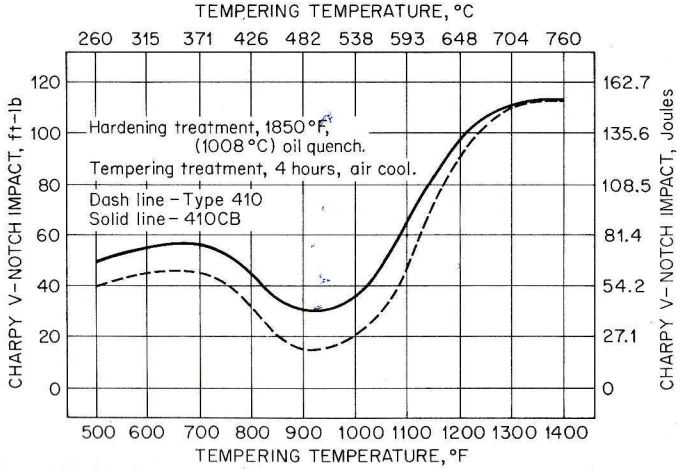

Fig. 31 Notch impact strengths of Types 410 and 410Cb stainless steels.[18]

TABLE 4

A_{c1} depression, °C per % alloy		M_s depression, °C per % alloy	
		(From 300°C)	
Nickel	−30	Carbon	−474
Manganese	−25	Manganese	−33
Cobalt	−5	Nickel	−17
Silicon	+20 −30	Chromium	−17
Aluminum	+30	Molybdenum	−21
Molybdenum	+25	Tungsten	−11
Vanadium	+50	Silicon	−11

of carbon and nitrogen. When done in air, surface decarburization is also possible. This could lead to unhardenable delta ferrite formation.

Over tempering, particularly with the nickel-containing grades, may result in nickel partitioning, forming reverted and enriched austenite which will be retained on cooling.

The last mechanism is the contamination of the surface with carbonaceous material which may be locally absorbed in heat treatment. This reemphasizes the usual stainless rule that the stock to be heat-treated must be clean.

The effect of retained austenite depends on percentage. The typical inadvertent amount encountered may range up to 25 to 30%. This amount may significantly reduce yield strengths to the austenitic level. Another potentially serious reaction can be the later martensitic transformation following tempering. This volume change could lead to cracking. The second of a double tempering is intended to temper any martensite formed in this manner. The use of a double temper is common in tool steel technology.

REFERENCES

1. Baerlecken, E., et al.: Investigations Concerning the Transformation Behavior, the Notched Impact Toughness and The Susceptibility to Intercrystalline Corrosion of Iron-Chromium Alloys with Chromium Contents to 30%, *Stahl Eisen*, vol. 81, no. 12, pp. 768–778, Jun. 8, 1961.
2. Bungardt, K., E. Kunze, and E. Horne: Structure of the System Fe-Cr-C, *Archiv Eisenhuettenwes.*, vol. 29, pp. 193–203, March 1958.
3. Johnson, C. R., and S. J. Rosenberg: Constitution Diagram for 16% Cr-2% Ni Stainless Steel, *Trans. Am. Soc. Met.*, vol. 55, pp. 277–286, 1962.
4. Nehrenberg, A. E., and P. Lillys: High Temperature Transformations in Ferritic Stainless Steels Containing 17-25% Chromium, *Trans. Am. Soc. Met.*, vol. 46, pp. 1176–1203, 1954.
5. Tisinai, G. F., and C. H. Samans: Phase Relationships and Mechanical Properties of Some Iron-Chromium Carbon-Nitrogen Alloys, *Trans. Am. Soc. Met.*, vol. 49, pp. 747–758, 1957.
6. Kaltenhauser, R. H.: Welding Maraging Stainless Steels, *Weld J., Res. Suppl.*, vol. 44, pp. 1–4, September, 1965.
7. Thielemann, R. H.: Some Effects of Composition and Heat Treatment on the High Temperature Rupture Properties of Ferrous Alloys, *Am. Soc. Test Mater. Proc.*, vol. 40, pp. 788–804, 1940.
8. Aggen, G.: U.S. Patent 3,650,731.
9. Irvine, K. J., D. J. Crowe, and F. B. Pickering: The Physical Metallurgy of 12% Chromium Steels, *J. Iron Steel Inst. London*, vol. 195, pp. 386–405, August, 1960.
10. Aggen, G.: Phase Transformations and Heat Treatment Studies of a Controlled-Transformation Stainless Steel Alloy, thesis submitted to Faculty of the Department of Metallurgical Engineering, Rensselaer Polytechnic Institute, August, 1963.
11. Dulis, E. J., et al.: Relationship Between Fatigue and Damping Characteristics and Microstructure of 12% Cr Steels, *Trans. Am. Soc. Met.*, vol. 54, pp. 456–465, 1961.
12. Link, H. S., and P. W. Marshall: The Formation of Sigma Phase in 13%-16% Chromium Steels, *Trans. Am. Soc. Met.*, vol. 44, pp. 549–559, 1952.
13. Banerjee, B. R., et al.: Ausworking T422 Stainless Steel, *Trans. Am. Soc. Met.*, vol. 56, pp. 629–642, 1963.
14. Westgren, R. C., and E. J. Dulis: Effects of Ausrolling on the Properties of Crucible 422 Stainless Steel, *ASTM STP 369*, pp. 8–15, 1963.
15. Hosoi, Y., and K. E. Pinnow: The Tensile Properties of Type 410 Stainless Steel Deformed Before and After Martensite Transformation, *Trans. Am. Soc. Met.*, vol. 53, pp. 591–602, 1961.
16. Floreen, S.: The Properties of Low Carbon Iron-Nickel Chromium Martensites, *Trans. Am. Inst. Min. Metall. Pet. Eng.*, vol. 236, pp. 1429–1440, 1966.
17. Hauser, J. J., et al.: Submicroscopic Structures in Tempering 410 Stainless Steel, *Trans. Am. Soc. Met.*, vol. 54, pp. 514–525, 1961.

18. Tanczyn, H.: Properties of 12% Chromium Alloys Modified With Small Columbium Additions, *ASTM STP 369*, pp. 80–87, 1963.
19. Tricot, R., and R. Castro: Study of the Isothermal Transformations in 17% Chromium Stainless Steels, *Met. Treat. London*, pp. 299–310, August, 1966.
20. McGannon, H. E. (ed.): "The Making, Shaping and Treating of Steel," 9th ed., pp. 1170, 1178, United States Steel Corp., Pittsburgh, Pa., 1969 (Copyright 1971, United States Steel Corp.)
21. "Republic Enduro Stainless Steels," p. 130, Republic Steel Corp., Cleveland, Ohio, 1951.
22. Roberts, G. A., J. C. Hamaker, Jr., and A. R. Johnson, "Tool Steels," p. 200, American Society for Metals, Metals Park, Ohio, 1962.